Journal of Materials and Engineering Structures

Research Paper

Damage estimation of low to medium rise reinforced concrete buildings considering vertical irregularity

Hemil M. Chauhan [a,*], ***Dr. Kaushal B. Parikh*** [b]

[a] *Research scholar,Gujarat technological university, Ahmedabad, Gujarat, India*

[b] *Professor and Head, Applied Mechanics Department, Govt.Engg.College, Dahod, Gujarat, India*

ARTICLE INFO

Article history :

Received : 03 February 2022

Revised : 22 January 2023

Accepted : 23 January 2023

Keywords:

Pushover analysis

Energy based damage index

Stiffness based damage index

Vertical irregular buildings

ABSTRACT

In current study, Damage estimation is carried out using new methodology using parameters such as absorbed energy and degrading stiffness by pushover analysis. A new stiffness-based damage index is developed for each increasing step of pushover analysis, which takes into account the cumulative effects of increasing each lateral load and displacement. Non-cumulative absorbed energy-based damage index is calculated using the pushover curve's first maximal hysteretic cycle. These suggested methods can be utilised to quickly calculate the global damage index for low to medium rise vertical irregular buildings. The proposed two methods are evaluated using three regular and vertical irregular buildings considering various parameters such as varying heights, setback orientations, plastic hinges and monotonic loads. Furthermore, existing deformation and strength-based damage indices are used to calibrate the proposed damage indices. Both proposed damage indices may calculate damage index at any point on the pushover curve, however the damage indices are computed at different performance levels. The research based on damage index showed that two approaches for evaluating damage to irregular buildings are easy to use and accurate, Also, using the results of pushover analysis, structural designers may estimate the global damage index as a performance criterion in short period of time.

1 Introduction

Structures in earthquake prone zones are likely to get damaged or collapse due to seismic instability during the occurrence, which is very unpredictable. As a result, the structural system should be built in such a way that the loss of life and property is mitigated. Deterioration of strength, stiffness, or ductility is the most common cause of structural damage. The IS code for force-based seismic design is presently in use, meaning that forces and displacements within elastic limits are computed and then combined to build structural parts [1]. It is uneconomical to design the structures that is earthquake-proof, yet every structures must be designed to resist earthquakes forces. As a result, engineers are allowed to certain structural damage in the event of an earthquake disaster. One of the key causes of structural damage during prior earthquakes

* *Corresponding author. Tel.: +91 9099013358.*
E-mail address: hemilcivil@gmail.com

e-ISSN: 2170-127X,

RESEARCH REVIEW of Sciences and Technologies

have been found to be irregular plan and elevation configurations of the buildings [2]. Deterministic and probabilistic approaches have been introduced by some researchers[3], the mathematical approach is used to compute the global damage index (GDI) might generate a distinction between deterministic and probabilistic indices. Many researchers are recommended the deterministic approach over the probabilistic approach because of its simplicity and capacity can be used in practical situation right away. Furthermore, they take substantially less time to compute than probabilistic indices[4]. Several researchers have proposed deterministic techniques based on numerous engineering demand parameters (EDP) [5-10]. In the relevant literatures, two primary methodologies were used to determine the structural damage value with proposing empirical formula. The first technique was based on a balance between a structure's demand and capacity, while the second method was based on degradation of EDPs such as stiffness, strength, and ductility, as well as the use of other EDPs. In the past, using single and multiple EDPs, researchers had developed several damage indices calculation methodologies for various structures. Zameeruddin et al. (2021) [11] had proposed damage index (DI) calculation techniques based on energy, stiffness, strength, and ductility parameters, and Vimala A. et al. (2014) [9] had proposed empirical formula to compute DI using dissipated energy, both studies were done on 2D regular frames with performing nonlinear static analysis on various performance levels. Habibi A. et al. (2012, 2016) [12, 13] had performed nonlinear dynamic analysis to compute absorbed energy, ductility, stiffness, and drift on 2D setback frames, while Ghobarah A. et al. (1999)[8] explored stiffness based DI, but these studies neglected the torsional impacts. S. Diaz et al. (2017) [14] has been addressed at damage estimation in terms of stiffness, ductility, and dissipated energy, although torsion and bidirectional moment effects were not considered in the investigation. Damage index estimation on different plan irregular buildings using several EDPs such as inter-storey drift, joint rotation, and peak displacement on normal structures was studied by Pritam H. et al., (2020-2019) [7, 15], and it was recommended to work out on ductility, dissipated energy, and stiffness parameters, though the authors did not account for torsional impacts in their study. Cinitha A. et al. (2015) [10] had introduced a fully elastic-plastic damage measure based on spectrum displacement and acceleration, as well as a time-period based softening damage index. M. Zameeruddin et al. (2017)[16] were used nonlinear static analysis in regular frames to develop a new empirical technique for estimating stiffness-based damage indices that took into account the cumulative impact of deteriorating stiffness and ignored torsion effects. Although S. Jeong et al. (2006) [17] had studied torsional and geometrical irregularities, but the application in high-rise buildings was unclear. Samir Tiachacht et al. (2021-2020) [18, 19] had proposed method for lactating and measuring structural damage that focuses on the modal strain energy ratio in conjunction with slime mould algorithm (SMA) and marine predators algorithm (MPA). Also had worked (2020) on new technique for damage detection in 3D frame structures using genetic algorithms (GA) combined with finite element modelling (FEM).

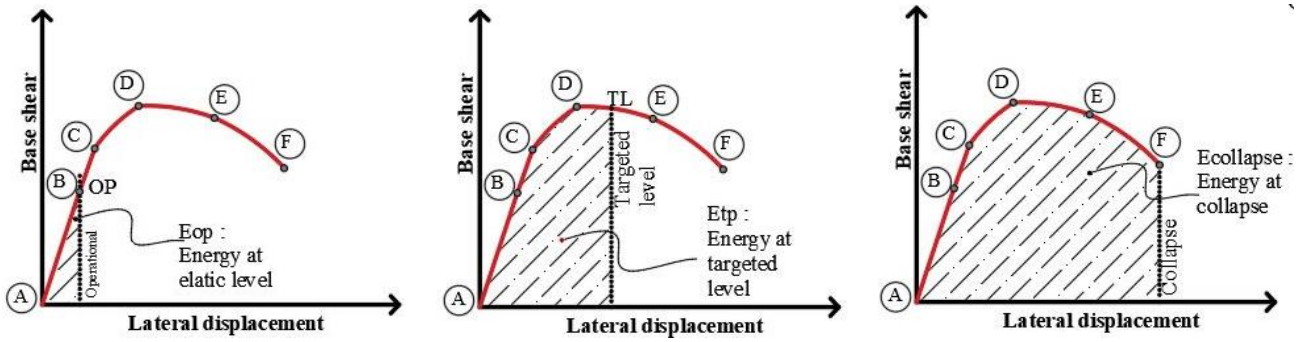

(a) (b) (c)

Fig. 1 – (a), (b) & (c) absorbed energy on critical points of curve

According to the series of studies, numerous DI estimation techniques based on nonlinear static and dynamic analysis have become accessible, however they were either difficult or ineffective when applied to irregular 3D structures. Several studies have found that structural damage is estimated using one or two parameters like stiffness, dissipated energy, ductility, rotation, inter-storey drift (IDR), and maximum lateral deformation, but it is preferable to estimate damage using multiple response parameters that describe the actual damage scenario of a structure under seismic conditions [20]. It was also determined that nonlinear dynamic analysis necessitates complicated mathematical computations that take a long time to analysis, as well as a number of ground motions data. As a result, the alternative method of nonlinear static analysis (pushover

analysis) has gained a lot of attention in the design industry since it takes less time and is easier to use than nonlinear time history analysis [21]. However, Samir Tiachacht et al. (2021–2022) [18, 19] has conducted a number of studies on damage estimation using a variety of composite materials, inverse analysis–based frame structures, laminated plates with various end conditions, and steel plates using frequency response function (FRF) and inverse analysis.

The constraints of previous research are examined in depth in this current research work, and damage indices are developed that is allowed pushover analysis to quantify the impacts of stiffness deterioration and energy dissipation after each incremental displacement. The primary goal of this research is to estimate the damage in terms of DI on low to medium rise RC regular and setback type of vertical irregular buildings. In order to make the DI estimate method more approachable and straightforward, a relationship is proposed between absorbed energy and degraded stiffness with lateral drift. These proposed methods may be used to quickly calculate the global damage index for low to medium rise vertical irregular buildings, while also taking into account the most important EDPs like absorbed energy and degraded stiffness, and simplifying the damage estimating procedure.

2 Damage estimation methods

The damage of structural elements, which occurs as a result of severe deformation and concrete becoming nonlinear, is the most common cause of partial or fully collapse in irregular RC buildings [21, 22]. Calculating the damage index of irregular buildings is critical due to the unpredictable nature of building reactions. The most essential criteria include strength, stiffness, ductility, lateral displacement (drift), torsion, and other EDPs can be used to characterize the failure process [5]. Modified stiffness-based damage indexes and energy-based damage indices are developed and applied to a wide range of irregular 3D buildings with considerable torsion-induced unanticipated response due to vertical irregularities in the current work. The majority of damage indices concentrated on flexural yielding in beams and columns. The recommended method can be applied to any type of plastic hinges that is subjected to nonlinear analysis. The advantages and limitations of the new damage indices (DIs) evaluation are given below.

Advantages

Damage can be estimated at any point of loading on the curve, rather than assuming the maximum displacement or deformation of the structure near collapse on the pushover curve.

- On different performance levels, the DI is appropriate for estimating structural stiffness variations and absorbed energy associated with the first hysteretic cycle.
- The recommended indices can be utilized to model damage induced by causes other than flexural yielding. All possible failure modes can be included in the models by using this approach.
- The degraded stiffness is estimated after each incremental step of the pushover analysis, and the DI is determined based on that, taking into consideration the cumulative effect of stiffness degradation.
- It is simple to use and just requires a few calculations, making it an excellent alternative to nonlinear time history analysis. Nonlinear time history analysis, which is complex, time-consuming, and requires a lot of ground motion data.

Limitations

- The limits of the pushover analysis technique have an impact on the applicability and accuracy of the suggested damage estimation.
- It demands correct nonlinear modelling; else, nonlinear results has become inappropriate.

2.1 Energy based damage index (EBDI)

The quantity of energy absorbed by the building is represented by the area under the pushover curve from the selected displacement or load. As demonstrated in figure 6, pushover curves are formed in both directions by applying monotonic loads in various patterns such as (uniform) acceleration, IS 1893-2016 (inverted triangle), and mode type (parabolic curve).

This area computing technique is integrated the cumulative cyclic loading effects without the need for non-linear dynamic analysis since it follows the collapse mechanism from the pushover curve. The inelastic energy in equation (1) indicates the multiple energies expended by permanent plastic rotations in beams and columns during dynamic loadings, showing the degree of damage. The area under the curve at different performance levels was estimated using the first hysteretic cycle as a pushover curve, in which the ideal quantity of various energies was absorbed through lateral load. As indicated in equation (2), damage is calculated as the ratio of the difference in absorbed energy at intended performance level and energy absorbed at elastic performance level to the difference in absorbed energy at ultimate displacement level and energy absorbed at elastic performance level.

$$E_i \text{ (input energy)} = E_e + E_d \tag{1}$$

Where, E_e (elastic strain energy) = E_k (kinetic energy) + E_s (strain energy), &

E_d (dissipated energy) = E_h (hysteretic energy) + E_ξ (viscous damping energy)

Figure 1a is indicated the absorbed energy at the operational level (E_{op}), which is defined as the area under the pushover curve up to its first yielding point. Energy at targeted performance point represented the energy absorbed by the structure up to any specified performance point when the damage is to be evaluated as shown in figure1b. The area covered up to the last lateral displacement point, as illustrated in figure 1c, is the structure's whole nonlinear energy capacity ($E_{collpase}$). (Area beneath the curve from the point of collapse) Figure 2 is depicted the fitting curve's polynomial equation which is used to compute energy at any point along the curve. Equation (2) is used to generate an energy-based damage index at a particular location on the pushover curve, and equation (3) is used to determine absorbed energy using 6-degree polynomial equation.

$$\text{Damage index } (D_{i\ \text{Energy}}) = \frac{E_{t.p} - E_{op.}}{E_{co.} - E_{op.}} \tag{2}$$

$$\text{Energy @ t.p} = \int_0^{S_{d\ (t.p)}} (ax^n + bx^{n-1} + C)\, dx \tag{3}$$

Where, $E_{(t.p)}$ targeted point = Absorbed energy at targeted performance level

$E_{op.}$ = Absorbed energy at operational level, & $E_{co.}$ = Absorbed energy at collapse level

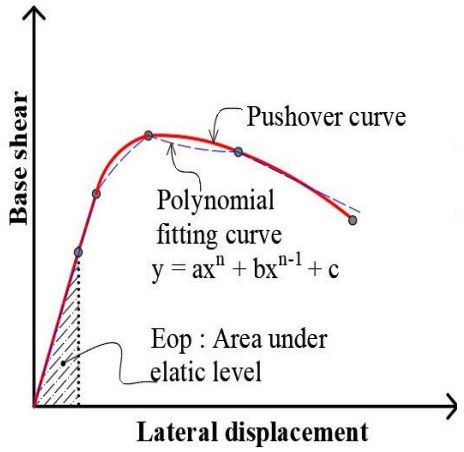

Fig. 2 – performance levels on pushover curve

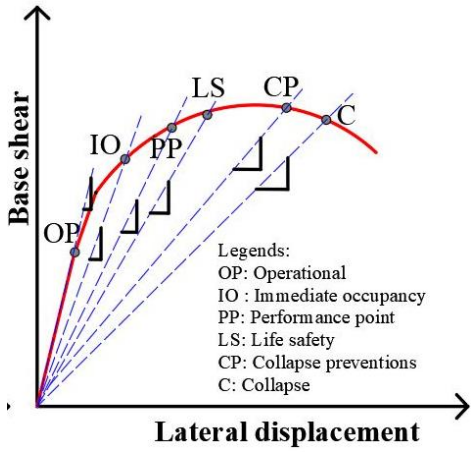

Fig. – 3 stiffness based nonlinear parameters

2.2 Stiffness (degradation) based damage index (SBDI)

In a pushover analysis, the structure's stiffness decreases with each incremental step and is influenced by a number of variables. Powell and Allahabadi (1988) [5] were the first to examine into the stiffness-based damage index using nonlinear time history analysis. Ghobarah et al.(1999) [8] had proposed a novel empirical method based on pushover and nonlinear time history analysis in 1999. However, due to some limitations, M. Zameeruddin et al.(2017) [16] had modified the approach

and used nonlinear static analysis to address the cumulative effects of stiffness degradation parameter, and that empirical formula is generally used for regular frames. The cumulative impacts of each incremental step were examined using new techniques in this study, and a suggested technique for degradation of stiffness with increasing lateral load was proposed.

It was observed during study when considering progressive stiffness degradation, two adjustments must be considered: the first at the plastic hinge placements and forms, and the second at the gradual member stiffness deterioration between two plastic hinges. The imposed monotonic lateral load and displacement are directly and inversely associated to the stiffness of a structure. At each performance level, the initial slope is used to determine stiffness. As shown in figure 3, nonlinear components depending on stiffness are used in the computation. Equation (4) is proposed to compute a stiffness-based damage index at a given displacement on the pushover curve. The pushover curve indicates how a structure's capacity degrades with increasing displacement, demonstrating that stiffness deterioration also follows the similar sequence. This leads us to conclude that the damage calculated using formulae given by researcher M. Zameeruddin et al. (2017) [16] is for the initial yield of the structure. However, a quantification may result in an incorrect assessment of the behaviour of structures, while the structure still has reserve strength that was not used. Hence a novel idea has been proposed to get beyond the previous restrictions, and it includes the cumulative degrading stiffness as shown in equation 4.

$$DI_{k\,@\,t.p} = 1 - \frac{\sum V}{\sum K * d} \tag{4}$$

Where, DI_k, targeted point = Stiffness based damage index at targeted performance level

$\sum V$ = $V_1 + V_2 + V_3 + \text{---} + V_n$ (Summation of base shear up to targeted performance level)

$\sum K$ = $K_1 + K_2 + K_3 + \text{---} + K_n$ (Summation of stiffness up to targeted performance level)

Where, 1, 2, 3 -----n are the incremental lateral steps

d = Corresponding lateral displacement at targeted performance level

2.3 Performance based seismic design (PBSD)

A performance-based seismic design technique is used to evaluate a building's lateral deformation and damage tolerance for different performance levels and at a performance point [10, 22]. Different performance levels [22, 23] indicated specific seismic damage states that may or may not be satisfied under earthquake loads, such as operational (OP), immediate occupancy (IO), life safety (LS), collapse prevention (CP), and collapse (C). A conceptual flowchart for evaluating seismic performance of RC buildings in terms of damage index is shown in figure 4.

The most important aspect of defining performance targets in PBSD is defining design criteria, each performance target is given explicitly, and the indication is based on an acceptable risk of structural element's damage at predetermined plastic hinge positions at various levels of seismic hazard [24]. As shown in table 1, the various performance levels produced in PBSD are based on permanent and transient drift. To define the structure's performance level, nonlinear static and/or dynamic analysis is used to measure the inelastic response. Pushover analysis is a type of approximation performance-based seismic design technique with some constraints in terms of dynamic aspects like enhanced mode involvement, hysteresis loops, and so on [1]. The performance-based seismic design method's major goals are to predict and reduce damage to a structure that has been subjected to an earthquake. This technique consists of a range of procedures for designing a structure in a controlled manner so that its behaviour to seismic loading is ensured at predetermined performance levels [13].The pushover curve is converted into an acceleration displacement response spectrum (ADRS) in these cases, which shows the structure's seismic capacity as well as the performance point. The performance point, which is the intersection of the pushover curve and the response spectrum, is depicted in figure 5 as an ideal representation [25]. The pushover curve is well identified and appropriate findings were presented for regular structure without taking into account the torsion irregularities generated in structure[26].

The different performance levels are defined by FEMA 273/356 [20], ATC 40/58 [27], and SEOAC vision [25], as indicated in figure 3.

Table 1 - Different performance levels in available standard

FEMA 273/356 [20]	ATC 40/58 [27]	SEAOC vision 2000 [25]
Performance level	Projected damage	Expected performance
Immediate occupancy (IO)	Negligible	Fully operational
Damage control range (DCR)	Light	Operational
Life safety (LS)	Moderate	Life safe
Limited safety range (LSR)	Severe	Near collapse
Collapse prevention (CP)	Complete	Total collapse

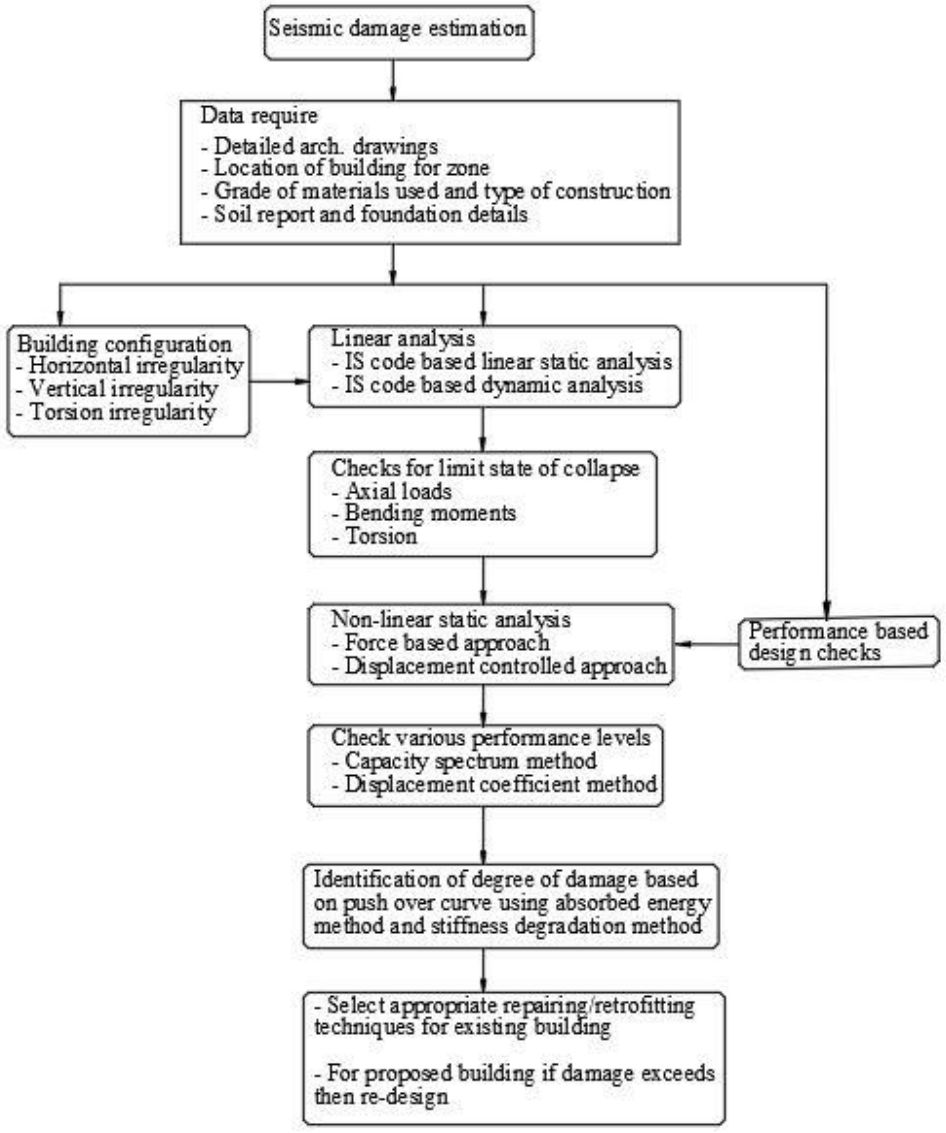

Fig. 4 – flow-chart for seismic damage evaluation in terms of damage index

The drift limitation of several performance levels are shown in table 2. In terms of lateral load or displacement, the various performance levels are shown below in ascending order. 1) Operational level (OP): This performance level is carried out until the structure reaches its elastic limit, at which point no damage occurs. The conclusions are essentially identical to

those of the linear analysis since it is just in the elastic limit. 2) Immediate occupancy (IO): This performance level exceeds the structure's elastic limit, resulting in nonlinear reaction, although it is still considered safe following an earthquake. After an earthquake, structures can be used immediately. 2a) Damage control range (DCR): This performance level is in the intermediate of the IO and LS performance levels. 3) Life safety (LS): This performance level is achieved when the strain hardening stage is reached and the damage range is within repairable limits. There is no damage allowed to people's lives. The most of the structures are designed to life safety level. 3a) Limited safety range (LSR): This performance level lies between LS and CP, and some repairable damage can occur at this level with total life safety. 4) Collapse prevention (CP): This performance level is well-suited to gravity loads after an earthquake, when the structure partially collapses in the elements but not completely (Serviceable even after some damages in elements). 5) Collapse (C): After an earthquake, this performance level is no longer usable and can no longer provide any life safety against gravity loads.

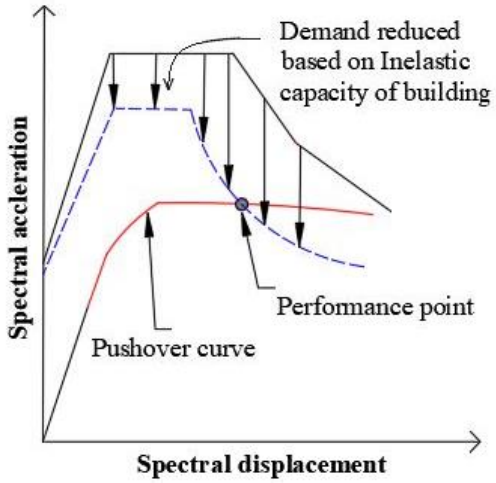

Fig. 5 – Idealized representation of performance point from ATC -40 [27]

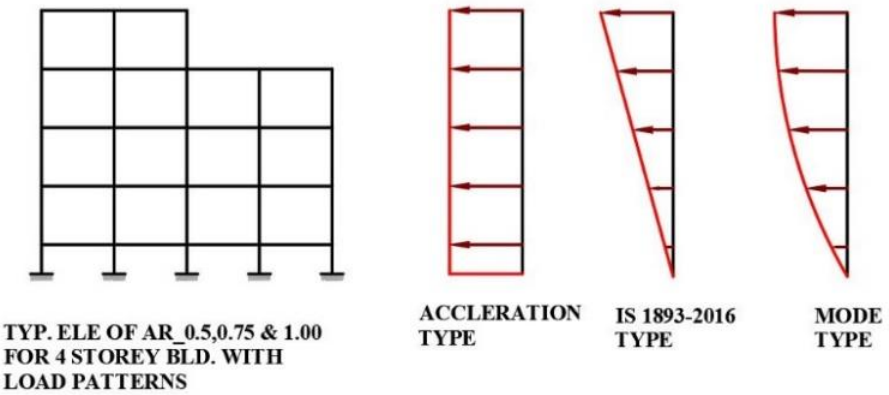

Fig. 6 – Monotonic Load patterns

Table 2 Drift limits at different performance levels [20, 27]

Performance levels	Description	Drift limits
Operational (OP)	Does not undergo any damage	< 0.7 %
Immediate occupancy (IO)	Elements are partially damage	1 %
Life safety (LS)	Remarkably damage of structural and nonstructural elements	2 %
Collapse prevention (CP)	Structural elements are about to collapse	4 %

3 Pushover analysis

The finite element formulation in pushover analysis is used to assess the incremental-iterative solution of the equilibrium equation (5) that is illustrated below. The lateral load is continuing applied to the building until a predetermined level is reached or failure in structural elements, whichever occurred earlier.

$$P = \mathrm{KU} \tag{5}$$

Where, P = incremental lateral load applied to the building

K = nonlinear stiffness matrix

U = lateral displacement of the building in the direction of load

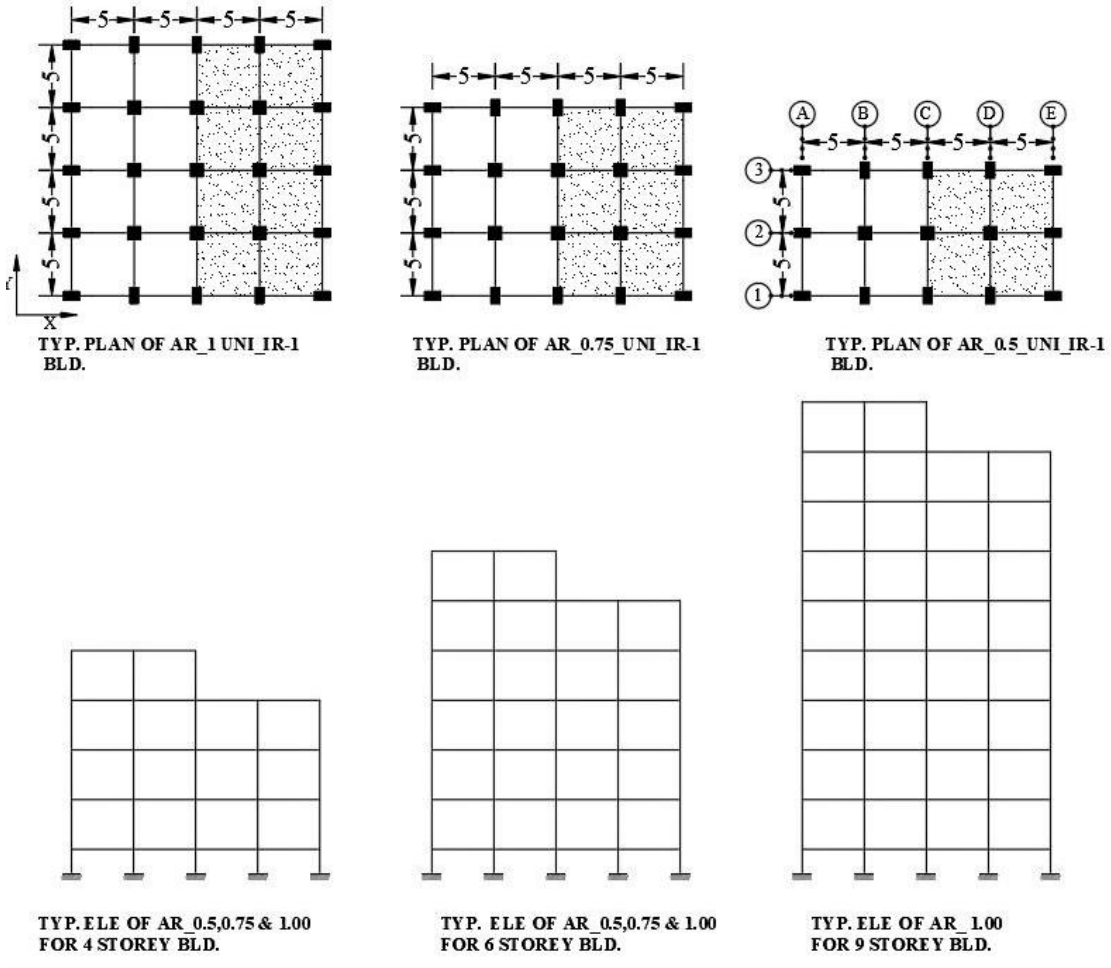

Fig. 7a – plans and elevations of 4, 6, and 9 storey buildings with unidirectional setback

3.1 Building example

The proposed DIs were applied to 4, 6, and 9 storey regular and vertical irregular RC buildings with unidirectional and bidirectional setbacks, as shown in figure 7a and 7b. Three distinct three-dimensional structures represent short, medium, and long time periods. The foundation and remaining floor heights are considered 2 and 4 meters, respectively. DIs were computed using a parametric analysis that took into account three different monotonic loadings, two setback directions, three different storey irregularities with considering variety of plastic hinges.

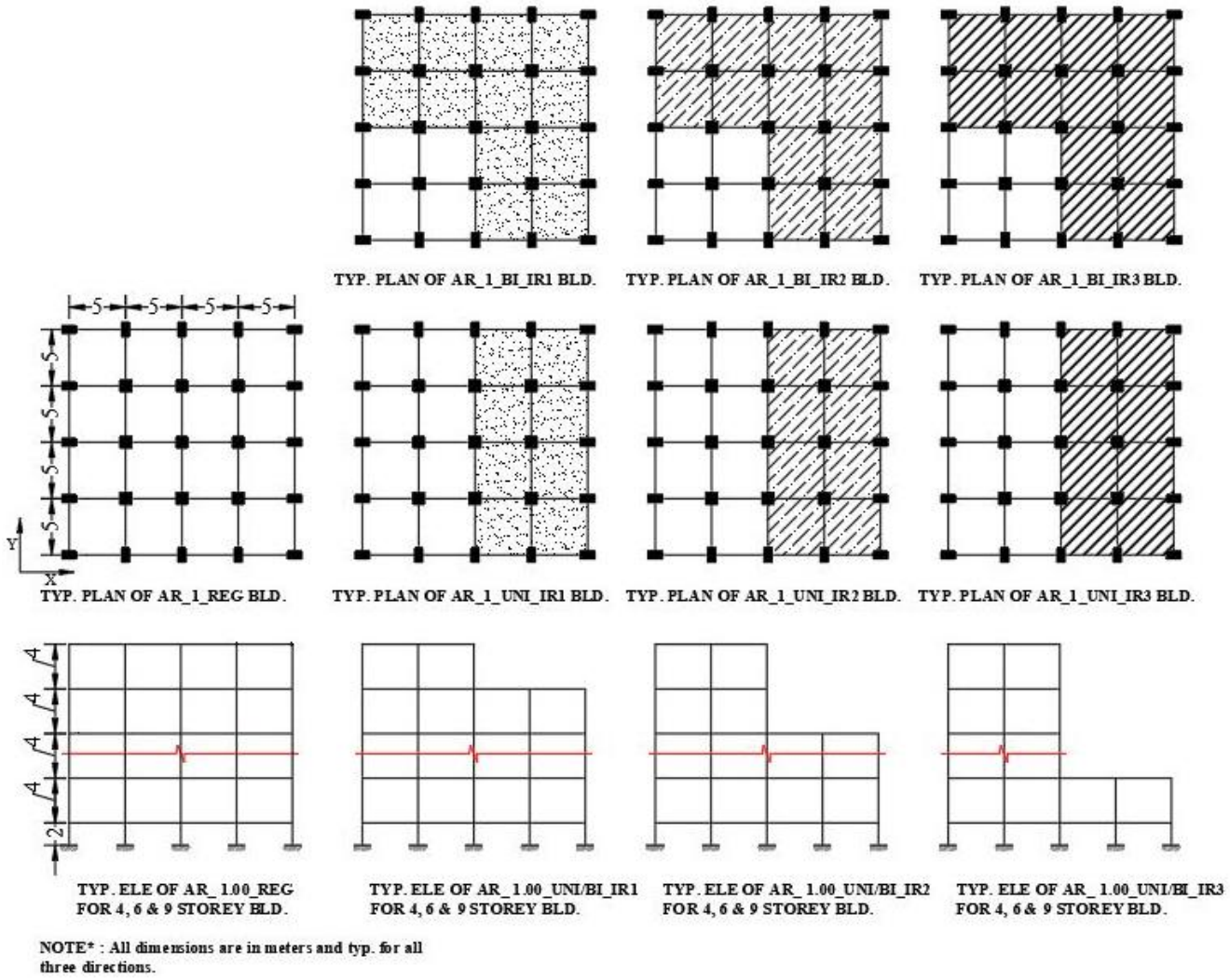

Fig. 7b – plans and elevations of 4, 6, and 9 storey regular and irregular buildings

Building examples are designated such as S4_0.5_UNI_IR1 X_UD, means four-story building with 0.5 plan aspect ratio, unidirectional setback type, one irregular storey (setback), X denotes horizontal direction and UD stands for user defined plastic hinges. For 4 and 6 storey buildings, rectangular (Exterior) columns of sizes 300 x 600 mm, and for 9 storey buildings 300 x 750 mm are assumed. For all buildings, 600 × 600 mm square (internal) columns sizes are considered, and beams sizes are used 230 x 450 mm for all levels of all buildings. Steel main bars and lateral ties with a yield strength of 415 MPa and concrete with a compressive strength of 25 MPa are used. The slab and floor finish dead loads are taken 3.75 kN/m^2 and 1.00 kN/m^2, respectively. On the external and interior beams, brick masonry wall thicknesses of 230 mm and 115 mm are employed, respectively. All slabs are subjected to a live load of 2 kN/m^2. The IS 456-2000 [28] and IS 1893-2016 [29] codes, which includes linear static and dynamic analysis, are used to design buildings. Seismic load is calculated using IS 1893-2016 [29], and linear analysis is done using medium soil strata using zone factor 0.16, importance factor 1, response reduction factor 5. IS 1893-2016 [29] recommends that structural parts such as beams and columns have a factored moment of inertia. As a result, the current study integrates the concept of a strong column and a weak beam.

3.2 Building modelling

The efficiency of nonlinear static methods is depended on the inelastic modelling of reinforced concrete sections. Plastic hinges are employed to present the reinforced concrete members' inelastic characteristics. According to performance-based seismic engineering, plastic hinges can be deformation-controlled (ductile action) or force-controlled (brittle action) (PBSE).

Plastic rotation constraints for reinforced concrete beams and columns are defined in PBSE standards. In current examples default and user defined deformation-controlled (ductile action) types of plastic hinges properties are assigned at 5% apart from beam column joints in the current investigation. User defined and default types of plastic hinges are used for buildings as shown in figure 7a and 7b, respectively. The maximum displacement for each RC structure was specified at 4% of the structure's height (ATC 40, 1996) [27]. The parameters of each plastic hinge are represented in the ideal force–deformation curve shown in figure 8. When the building is subjected to lateral loading, the most critical member reflects the worst-case scenario. The lateral seismic force distribution is calculated using acceleration, IS 1893[29], and mode forms of loading patterns for the pushover investigation. Figure 8 is shown a typical load–deformation relationship with a linear response from A to yield point B, followed by a linear response from B to C as stiffness decreases. In the absence of a definite experiment value, the slope from point B to point C can be assumed to be 0–10% of the starting slope, ignoring the effects of vertical loads acting through lateral displacements. The ordinate of point C represents the member's maximum strength, whereas the D coordinate represents the deflection at which considerable strength loss occurs. The remaining structural strength is shown by line DE.

Pushover analysis is used in the current study to determine the structural capacity to dissipate energy and degrading stiffness against the incremental lateral loading. Initially, gravity loads are applied to three-dimensional models that comprises bilinear load-deformation diagrams for all lateral force resisting parts. Then, a lateral load pattern that is predetermined and dispersed throughout the building height is used. In order to yield some members, the lateral stresses are increased. After modifying the structural model to take into account the reduced stiffness of the yielded members, the lateral forces are again increased until the additional members yield. The SAP2000 is used to perform an event-to-event solution technique. At the conclusion of each step in a pushover analysis, the control parameters "Iteration Tolerance" and "Maximum Iteration/Step" are used to check static equilibrium. The capacity of the hinge decrease during pushover analysis and it approaches the negative-sloped region of its force-displacement curve, which represents the nonlinear behaviour of a frame element.

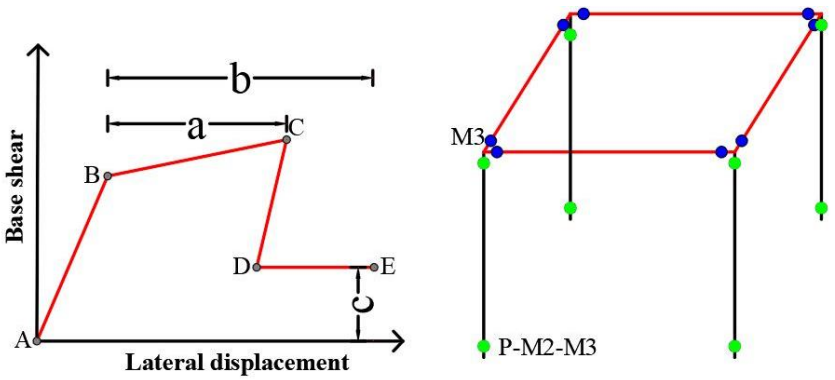

Fig. 8 – standard force-deformation curve and hinges details

4 Results and discussion

During the evaluation of the current work, the torsion induced by the setback type of vertical irregularity in the building and that causes unanticipated responses. The results of the pushover analysis for verification are almost identical to those of M. Zameeruddin's (2016) [1] research paper's 2D frame example.

Damage is assessed using standard 174 pushover curves of variety of the buildings at various performance levels of the curve. Figures 9 and 10 are shown the conventional pushover curve and the stiffness degradation curve of Storey 9 with considering default type of plastic hinges. Figures 11 and 12 are shown sample graph of drift versus energy based DI and drift versus stiffness based DI out of 116 graphs, which were generated to investigate the overall behaviour of a variety of buildings. The first hysteretic cycle for various energies and initial and secant stiffness at various performance levels is used to estimate damage. Both DIs are validated using existing nonlinear static analysis methods developed by Powell and Allahabadi (1988) [5] and Zameeruddin and K. Sanghle (2017) [16]. Both of the suggested damage indicators have shown

positive outcomes. The building example result of pushover analysis for the S4_0.5_UNI_ IR1_UD _ Acceleration- X dir._ case is presented in Table 3. Tables 4 and 5 have provided examples of EBDI and SBDI calculations for the S4_0.5_UNI_ IR1_UD_ Acceleration load type of building various performance levels, while table 6 is shown damage indices findings of different performance levels. Table 8 is shown the minimum and maximum drift limitations, which are well within the permitted limits as stated in table 2. In comparison to 9 storey structures, bidirectional setback types of 4 and 6 storey buildings exhibit sensitive responses.

Table 3 Pushover result for S4_AR_0.5_UNI_IR1_UD_ Accl_X

Step no.	Disp. (mm)	Base Shear (kN)	Number of hinges in particular range of performance levels							
			A-B	B-IO	IO-LS	LS-CP	CP-C	C-D	D-E	Beyond E
0	0	0	308	0	0	0	0	0	0	0
1	0.720	10.124	308	0	0	0	0	0	0	0
65	46.80	658.084	307	1	0	0	0	0	0	0
109	78.48	959.858	267	39	2	0	0	0	0	0
261	187.92	1309.105	200	30	77	1	0	0	0	0
323	232.56	1389.947	195	12	63	37	0	0	1	0
530	381.60	1571.625	193	8	20	4	0	0	82	1

Table 4 - Energy based damage index calculation for S4_AR_0.5_UNI_IR1_UD_ Accl_X

Step no.	Disp. (mm)	Base Shear (kN)	Per. level	Region	Drift (%)	Area under curve (kN-m)	Energy based damage index (%)	Remarks
0	0	0	-	-	0.000	-	-	Total 308 hinges
1	0.72	10.124	OP	A-B	0.004	-0.037	0.00	First step of Elastic range
64	46.08	647.959	OP	A-B	0.256	-2.376	0.00	Last step of Elastic range
65	46.80	658.084	IO	B-IO	0.260	-2.413	0.40	First hinge formation
72	51.87	722.406	P.P	IO-LS	0.288	-2.639	2.87	P.P @ IO-LS
109	78.48	959.858	LS	IO-LS	0.436	-4.021	17.93	Hinge @ IO-LS
261	187.92	1309.105	CP	LS-CP	1.044	-9.418	76.77	Hinge @ LS-CP
323	232.56	1389.947	C	CP-C-D-E	1.292	-11.55	100.00	Hinge @ D-E

For 4, 6, and 9 storey typical regular buildings with plan aspect ratio 1.00 and default plastic hinges, the maximum energy-based DI at the performance point (P.P) is roughly 8.47 %, 7.58 %, and 10.38 %, respectively. For 4, 6, and 9 storey irregular unidirectional setback with AR 1.00 types of buildings, the maximum EBDI values are adjusted to 17.6%, 11.34 %, and 8.20%, respectively. For bidirectional setbacks are taken into account, the values EBDI of three different structures are changed to 12.5%, 20.21 %, and 14.89 %, respectively.

For regular buildings of all three heights, the maximum stiffness-based DI at the P.P ranges from 40% to 45%. For 4, 6, and 9 storey buildings, these numbers are changed to 33.3% to 41.9%, 37.5% to 45.4%, and 42.9% to 45.4%, respectively, for unidirectional buildings. When examining bidirectional setback types of buildings, values range from 25 % to 37.8%, 33.3% to 42.3%, and 33.3 to 45.8% for 4, 6, and 9 storey buildings, respectively.

Table 5 - Stiffness based damage index calculation for S4_AR_0.5_UNI_IR1_UD_ Accl_X

Step no. (1)	Drift (%) (2)	Stiffness (kN) (3)	Cumulative base shear, $\sum K_o \times d_c$ (kN) (4)	Sum. of base shear, $\sum V$ (kN) (5)	Ratio of col.5/ col.4 (%) (6)	Stiffness based damage index (%) (7)	Remarks
1	0.004	14061.11	10.124	10.124	1.00	0.00	First step of Elastic range
65	0.260	14061.62	42775.417	21716.760	50.77	49.23	First hinge formation
72	0.288	13935.30	52640.575	26583.315	50.67	49.33	P.P @ IO-LS
109	0.436	12230.60	117713.407	58406.346	49.62	50.38	Hinge @ IO-LS
261	1.044	6966.28	541622.700	235964.161	43.57	56.43	Hinge @ LS-CP
323	1.292	5976.72	763074.193	319764.867	41.90	58.10	Hinge @ D-E

Table 6 - Damage indices at performance levels on curve of S4_AR_0.5_UNI_IR1_UD_Accl_X

Performance level	S_d (mm)	Drift (%)	Di_E (%)	Di_K (%)	$Di_{P\&A}$ (1988) (%)	$Di_{Z\&K}$ (2017) (%)
OP	46.080	0.256	0.00	0.00	0.00	0.00
IO	46.800	0.260	0.40	49.23	0.39	46.96
P.P	51.236	0.285	2.87	49.33	2.76	51.62
LS	78.480	0.436	17.93	50.38	17.37	68.83
CP	187.920	1.044	76.77	56.43	76.07	94.14
C	232.560	1.292	100.00	58.10	100.00	100.00

Di_E = Energy based damage index, Di_k = Stiffness based damage index

$Di_{P\&A}$ = Powell & Allahabadi's *deformation based damage index* (1988) [5]

$Di_{Z\&K}$ = Zameeruddin & K. Sanghle's *strength based damage index* (2017) [16]

In all scenarios, a performance point is attained that is well within the drift limit of the damage control range (DCR) level. The performance point is achieved in all circumstances when the stiffness damage index is extended about 50%, as shown in table 7. The majority results are almost matching but some results are deviated. It may be due to use of single engineering demand parameter (energy). The building sustained further damage when the stiffness deteriorated as a result of the pushover analysis. As the building's height rises, there is no noticeable change in drift range for any load patterns. The comparison to the acceleration type of load with IS 1893 and the mode type of load patterns, the mode type of load patterns have a greater drift.

In 4-story buildings cases with an aspect ratio (AR) of 0.5, the drift limit at the performance point is roughly 0.285 % to 0.376 % and 0.331 % to 0.454 % in the x and y directions, respectively, for all three load situations. The energy-based DI range was 0 % to 4.82 % in the x direction and 0 % to 7.80 % in the y direction. Drift is about the same in aspect ratios (AR) 0.75 and 1.00 as in 0.5 AR, however the energy-based DI ranges have been changed to 1.93 % to 5.16 % and 0 % to 3.95 % in the x direction and 4.04 % to 8.30 % and 0 % to 4.66 % in the y direction, for plan aspect ratios 0.75 and 1.00 respectively.

Table 7 - Damage indices at performance point

Sr. No.	Storey_ AR_ UD_IR1	Lateral loading type	S_d (mm)	Di_E (%) Proposed	Di_D (%) P&A(1988) Existing	Error of energy based DI (%)	Di_K (%) Proposed	Di_V (%) Z&K(2017) Existing
1	S4_0.5_UD_X	Accl.	51.24	2.87	2.76	3.99	49.33	51.62
2		IS-1893	67.70	0.00	0.00	0.00	49.47	49.29
3		Mode-2	59.07	4.82	4.66	3.43	49.46	57.77
4	S4_0.5_UD_Y	Accl.	59.53	5.73	4.44	29.05	49.44	51.26
5		IS-1893	81.79	0.00	0.00	0.00	49.56	45.62
6		Mode-1	76.70	7.80	7.57	3.04	49.69	52.92
7	S4_0.75_UD_X	Accl.	51.31	1.93	1.86	3.76	49.31	50.31
8		IS-1893	63.98	5.16	4.99	3.41	49.55	61.81
9		Mode-2	58.94	4.00	3.88	3.09	49.44	57.17
10	S4_0.75_UD_Y	Accl.	57.67	4.04	3.92	3.06	49.41	50.86
11		IS-1893	74.63	8.30	8.09	2.60	49.69	61.07
12		Mode-1	73.63	6.11	5.92	3.21	49.58	50.43
13	S4_1.00_UD_X	Accl.	51.39	1.93	1.86	3.76	49.31	50.87
14		IS-1893	67.26	0.00	0.00	0.00	49.46	49.91
15		Mode-2	58.88	3.95	3.82	3.40	49.44	58.18
16	S4_1.00_UD_Y	Accl.	56.31	3.44	3.34	2.99	49.39	51.43
17		IS-1893	75.82	0.00	0.00	0.00	49.52	47.36
18		Mode-1	70.82	4.66	4.51	3.33	49.52	49.40
19	S6_0.5_UD_X	Accl.	77.08	6.78	6.42	5.61	49.43	55.34
20		IS-1893	103.45	0.00	0.00	0.00	49.50	35.63
21		Mode-2	87.65	9.19	8.82	4.20	49.62	61.14
22	S6_0.5_UD_Y	Accl.	87.29	8.12	7.73	5.05	49.62	56.67
23		IS-1893	123.55	0.00	0.00	0.00	49.58	40.48
24		Mode-1	116.15	14.98	14.46	3.60	50.05	60.29
25	S6_0.75_UD_X	Accl.	77.19	5.68	5.36	5.97	48.76	55.32
26		IS-1893	103.62	0.00	0.00	0.00	49.49	35.73
27		Mode-2	94.55	0.00	0.00	0.00	49.45	34.84
28	S6_0.75_UD_Y	Accl.	84.78	8.00	7.62	4.99	48.90	55.80
29		IS-1893	118.49	0.00	0.00	0.00	49.56	36.19
30		Mode-1	12s0.86	0.00	0.00	0.00	49.57	37.33
31	S6_1.00_UD_X	Accl.	77.03	5.34	5.03	6.16	48.63	54.64
32		IS-1893	98.97	27.33	26.41	3.48	50.12	61.82
33		Mode-2	87.37	8.08	7.75	4.26	49.07	61.48
34	S6_1.00_UD_Y	Accl.	82.96	7.06	6.74	4.75	48.84	57.23
35		IS-1893	111.07	27.87	27.23	2.35	49.64	60.16
36		Mode-1	108.51	12.29	11.91	3.19	49.27	57.64
37	S9_0.5_UD_X	Accl.	115.97	12.05	11.15	8.07	48.95	64.68
38		IS 1893	144.93	35.92	35.13	2.25	49.69	71.30
39		Mode-2	130.95	14.00	13.34	4.95	49.21	68.98
40	S9_0.5_UD_Y	Accl.	128.52	13.17	12.40	6.21	49.21	64.54
41		IS 1893	168.21	33.60	32.98	1.88	49.87	71.55
42		Mode-1	168.79	19.30	18.77	2.82	49.83	67.91

43	S9_0.75_UD_X	Accl.	115.51	11.92	10.52	13.30	48.99	63.65
44		IS 1893	158.60	0.00	0.00	0.00	49.04	31.63
45		Mode-2	130.20	13.66	12.70	7.56	49.31	67.85
46	S9_0.75_UD_Y	Accl.	124.50	13.33	12.33	8.11	49.16	65.01
47		IS 1893	176.75	0.00	0.00	0.00	49.14	35.42
48		Mode-1	162.71	18.10	17.64	2.61	49.61	66.89
49		Accl.	114.03	12.89	8.10	59.14	48.96	60.01
50	S9_1.00_UD_X	IS 1893	155.43	0.00	0.00	0.00	49.02	31.95
51		Mode-2	128.48	12.17	10.33	17.81	49.23	64.21
52	S9_1.00_UD_Y	Accl.	120.44	12.34	10.41	18.54	49.08	62.39
53		IS 1893	168.86	0.00	0.00	0.00	49.09	31.78
54		Mode-1	155.10	15.45	14.97	3.21	49.51	64.91

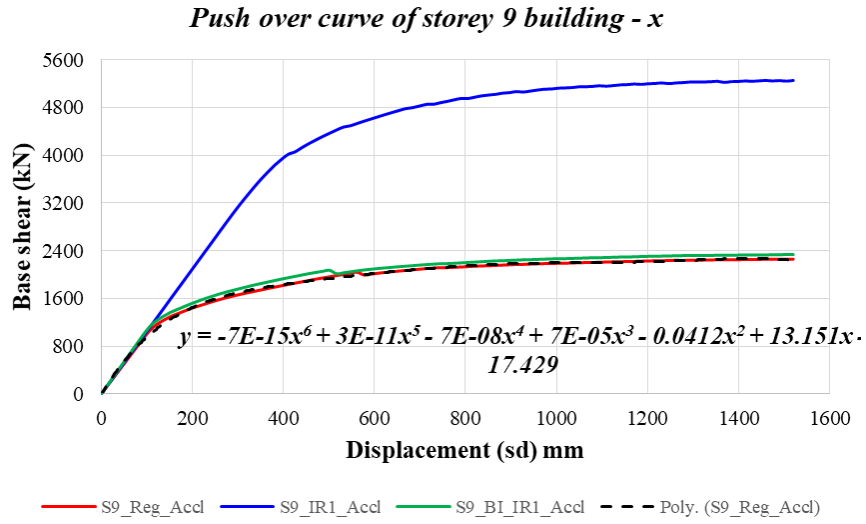

Fig. 9 – Pushover curve for different storey 9 building case

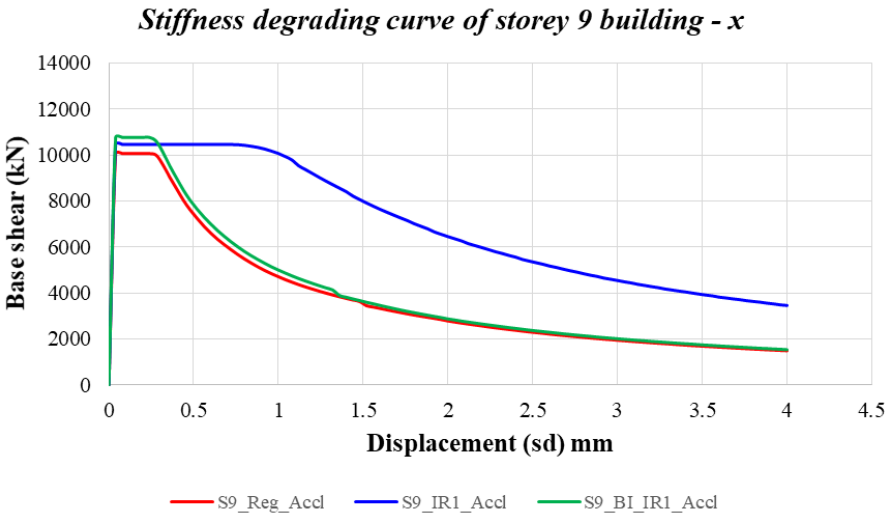

Fig. 10 – Stiffness degradation curve for different storey 9 building case

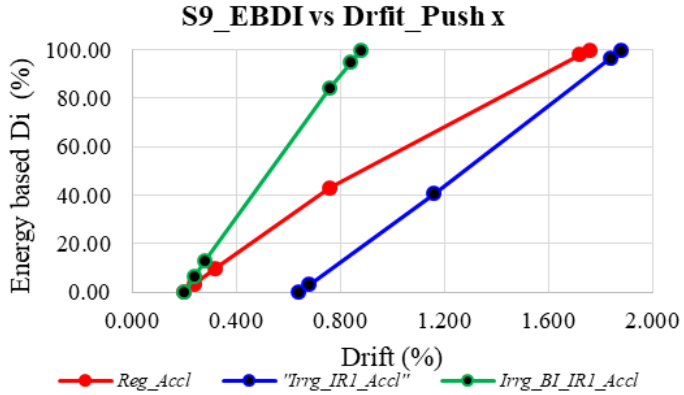

Fig. 11 – EBDI vs. Drift for various S9 buildings

Table 8 - Different minimum to maximum ranges at performance point against three lateral loads

Building type, Setback, with default types of plastic hinge	Storey	Drift range %		EBDI range %		SBDI range %	
		X direction	Y direction	X direction	Y direction	X direction	Y direction
Regular	4	0.200	0.200	3.44-8.14	0.79-8.47	40.0-40.3	40.0-40.3
Irreg_Uni_IR1		0.200	0.20-0.24	3.23-8.06	2.07-11.1	40.0-40.2	40.0-41.9
Irreg_Uni_IR2		0.120	0.12-0.16	7.67-13.3	5.51-17.6	34.0-34.3	33.4-38.8
Irreg_Uni_IR3		0.120	0.12-0.16	9.90-14.1	5.40-5.46	33.3-33.4	33.3-37.5
Irreg_BI_IR2		0.08-0.12	0.04-0.12	0.00-12.5	0.00	25.0-33.3	0.00-37.8
Irreg_BI_IR3		0.08-0.12	0.04-0.12	8.61-9.95	0.00-6.84	25.0-33.3	25.0-33.3
Regular	6	0.32-0.36	0.32-0.36	5.21-6.95	5.64-7.58	43.9-44.7	43.9-44.8
Irreg_IR1		0.20	0.20	11.31-11.34	10.16-10.92	40.3	40.3
Irreg_IR2		0.32-0.40	0.36-0.44	0.00	0.00	43.7-45.0	37.5-45.4
Irreg_IR3		0.28-0.36	0.32-0.40	2.20-7.43	4.47-4.75	42.8-44.6	43.7-45.1
Irreg_BI_IR1		0.2-0.24	0.2-0.24	5.93-6.51	0.00-5.45	40.0-41.8	40.0-41.7
Irreg_BI_IR2		0.12	0.16-0.20	6.52-7.01	11.42-11.91	33.3	37.8-40.3
Irreg_BI_IR3		0.12-0.16	0.16-0.24	4.82-10.92	4.15-20.21	33.3-37.7	37.5-42.3
Regular	9	0.32-0.36	0.32-0.36	7.64-9.90	8.48-10.38	44.0-45.0	44.1-45.0
Irreg_IR1		0.32-0.40	0.36-0.44	0.00	0.00	43.7-45.0	44.4-45.4
Irreg_IR2		0.28-0.36	0.32-0.44	0.00-7.24	0.00-7.26	42.9-44.7	43.9-45.4
Irreg_IR3		0.28-0.36	0.32-0.40	4.65-5.80	5.87-8.20	42.9-44.6	43.9-45.2
Irreg_BI_IR1		0.28-0.36	0.32-0.36	8.28-14.57	7.01-11.77	42.9-45.3	43.8-44.8
Irreg_BI_IR2		0.28-0.40	0.12-0.40	7.19-14.89	0.00-7.12	43.0-46.3	33.3-45.5
Irreg_BI_IR3		0.28-0.40	0.04-0.40	5.82-10.55	0.00-6.42	42.9-45.8	0.00-45.1

The drift limit at performance point in a 6-story structure with an aspect ratio (AR) of 0.5 is determined to be 0.296 % to 0.398 % in the x and 0.336 % to 0.475 % in the y directions for all three load situations. The energy-based DI ranges from 0% to 9.19 % in the x direction and 0% to 14.98 % in the y direction, respectively. The drift is nearly identical in aspect ratios

(AR) 0.75 and 1.00 as it is in 0.5 AR, but the energy-based DI range for AR 0.75 and 1.00 has been adjusted to 0% to 5.68 % and 5.34 % to 27.33 % in the x direction and 0% to 8% to 7.06 % to 27.87 % in the y direction, respectively.

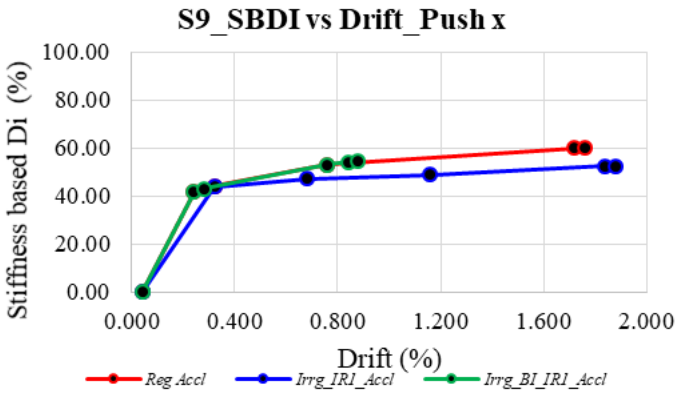

Fig. – 12 SBDI vs. Drift for various S9 buildings

The drift limit at performance point is shown in a 9-story structure with all aspect ratios, just as it is in a 6-story building, for all three load situations. However, with 0.5 AR, the energy-based DI range in the x and y directions is changed to 12.05 % to 35.92 % and 13.17 % to 33.60 %, respectively. The energy-based DI range is changed to 0 % to 13.66 % and 0 % to 12.89 % in the x direction, and 0 % to 18.10 % and 0 % to 15.34 % in the y direction for aspect ratios of 0.75 and 1.00, respectively.

5 Conclusions

The seismic performance of RC structures with regular and irregular geometry in plan using Indian seismic codes was investigated using linear static and dynamic analysis, followed by nonlinear static analysis utilising three distinct types of monotonic loadings. There have been several attempts to estimate seismic damage indices, but the majority of them were based on regular or irregular 2D frames and that did not respond well to unanticipated effects caused by irregularities. The current study is focused on 3D vertical irregular structures and it indicates that torsion caused an unexpected nonlinear reaction, as well as making the building more vulnerable to torsion. From this study, the following findings may be derived.

In present study, global damage index is found using two engineering demand parameters such as absorbed energy and degrading stiffness while gradually increasing lateral loads considering vertical irregularity. The study of 3D vertical irregular buildings yielded acceptable results and both DI approaches have been shown to accurately estimate the damage to 3D irregular buildings. The proposed damage indices can be used for the evaluation of damage at any displacement or force corresponding to the pushover curve. In push over analysis, load patterns are the most important elements in absorbed energy and stiffness deterioration. All three forms of monotonic load patterns should be used when evaluating damage at the point of performance. At any point along the pushover curve, global damage index can be estimated using proposed empirical formula. It is significantly more appropriate and efficient to estimate the damages for existing and prospective irregular structures at any point along the curve. The proposed stiffness damage index can calculate the damage value at the intended performance levels, accounting for all nonlinear responses at each incremental step of the pushover and the cumulative effects of degrading stiffness that were previously unaccounted for by existing damage estimations. The findings of the pushover curve in all cases show that the drift is substantially within existing standards' permitted limits. Although the force-based design approach based on Indian seismic code appears to work for regular frames. It fails to fulfil the life safety performance level standards in irregular frames with setbacks along their height. Short buildings with unidirectional and bidirectional setbacks, in particular induced a vulnerable reaction, necessitating greater design attention in order to attain a high degree of life safety performance. The majority of the setback buildings had already collapsed and or major damaged due to earthquakes events. As a consequence, it appears that code 1893-2016 criteria need to be revised in order to find and offer alternative indicators and techniques for predicting seismic response of vertically irregular structures.

Compliance with ethical standards

Conflict of interest: On behalf of all authors, the corresponding author states that there is no conflict of interest.

Acknowledgement

The research described in this paper was not financially supported by any organization.

REFERENCES

[1]- M. Zameeruddin, K.K. Sangle, Review on Recent developments in the performance-based seismic design of reinforced concrete structures. Structures, 6 (2016) 119-133. doi:10.1016/j.istruc.2016.03.001.
[2]- A.R. Habibi, K. Asadi, Seismic performance of reinforced concrete moment resisting frames with setback based on Iranian seismic code. International Journal of Civil Engineering, 12(1) (2014) 41-54.
[3]- A.J. Kappos, G. Panagopoulos, Performance-based seismic design of 3D R/C buildings using inelastic static and dynamic analysis procedures. ISET Journal of earthquake Technology, 41(1) (2004) 141-158.
[4]- A.J. Kappos, Seismic damage indices for RC buildings: evaluation of concepts and procedures. Progress in Structural Engineering and Materials, 1(1) (1997) 78-87. doi:10.1002/pse.2260010113.
[5]- G.H. Powell, R. Allahabadi, Seismic damage prediction by deterministic methods: Concepts and procedures. Earthquake Engineering & Structural Dynamics, 16(5) (1988) 719-734. doi:10.1002/eqe.4290160507.
[6]- M.V. Mohod, Pushover analysis of structures with plan irregularity. J Mech Civ Eng, 12(4) (2015) 46-55.
[7]- P. Hait, A. Sil, S. Choudhury, Damage Assessment of Reinforced Concrete-Framed Building Considering Multiple Demand Parameters in Indian Codal Provisions. Iranian Journal of Science and Technology, Transactions of Civil Engineering, 44(1) (2020) 121-139. doi:10.1007/s40996-020-00380-2.
[8]- A. Ghobarah, H. Abou‐Elfath, A. Biddah, Response‐based damage assessment of structures. Earthquake Engineering & Structural Dynamics, 28(1) (1999) 79-104.
[9]- A. Vimala, R.P. Kumar, C. Murty, Expended energy based damage assessment of RC bare frame using nonlinear pushover analysis. Urban Safety of Mega Cities in Asia, (2014).
[10]- A. Cinitha, P. Umesha, N. R Iyer, N. Lakshmanan, Performance-based Seismic Evaluation of RC Framed Building. Journal of The Institution of Engineers (India): Series A, 96(4) (2015) 285-294. doi:10.1007/s40030-015-0129-8.
[11]- M. Zameeruddin, K.K. Sangle, Damage assessment of reinforced concrete moment resisting frames using performance-based seismic evaluation procedure. Journal of King Saud University - Engineering Sciences, 33(4) (2021) 227-239. doi:10.1016/j.jksues.2020.04.010.
[12]- A.R. Habibi, M. Izadpanah, New method for the design of reinforced concrete moment resisting frames with damage control. Scientia Iranica, 19(2) (2012) 234-241. doi:10.1016/j.scient.2012.02.007.
[13]- A. Habibi, K. Asadi, Development of Drift-Based Damage Index for Reinforced Concrete Moment Resisting Frames with Setback. International Journal of Civil Engineering, 15(4) (2017) 487-498. doi:10.1007/s40999-016-0085-3.
[14]- L.P. S. Diaz, A. Barbat and Y. Vargas, , Energy damage index based on capacity and response spectra. Engineering Structures, 152 (2017) 424-436. doi:10.1016/j.engstruct.2017.09.019.
[15]- P. Hait, A. Sil, S. Choudhury, Damage assessment of reinforced concrete buildings considering irregularities (research note). International Journal of Engineering, 32(10) (2019) 1388-1394. doi:10.5829/ije.2019.32.10a.08.
[16]- M. Zameeruddin, K. Sangle, Seismic damage assessment of reinforced concrete structure using non-linear static analyses. KSCE Journal of Civil Engineering, 21(4) (2017) 1319-1330. doi:10.1007/s12205-016-0541-2.
[17]- S.-H. Jeong, A.S. Elnashai, New Three-Dimensional Damage Index for RC Buildings with Planar Irregularities. Journal of Structural Engineering, 132(9) (2006) 1482-1490. doi:10.1061/(ASCE)0733-9445(2006)132:9(1482).
[18]- Samir Tiachacht, Samir Khatir, Cuong Le Thanh, Ravipudi Venkata Rao, Seyedali Mirjalili, Magd Abdel Wahab, Inverse problem for dynamic structural health monitoring based on slime mould algorithm. Engineering with Computers, 38 (2021) 2205-2228. doi:10.1007/s00366-021-01378-8.
[19]- S. Tiachacht, A. Bouazzouni, S. Khatir, A. Behtani, Y.-L.-M. Zhou, M.A. Wahab, Structural health monitoring of 3D frame structures using finite element modal analysis and genetic algorithm. JOURNAL OF

VIBROENGINEERING, 20(1) (2018) 202-214. doi:10.21595/jve.2017.18571.
[20]- FEMA 273, NEHRP guidelines for the seismic rehabilitation of buildings; FEMA 274, Commentary. Washington (DC): Federal Emergency Management Agency. (1996).
[21]- S. Khatir, M. Abdel Wahab, S. Tiachacht, C. Le Thanh, R. Capozucca, E. Magagnini, B. Benaissa, Damage identification in steel plate using FRF and inverse analysis. FRATTURA ED INTEGRITA STRUTTURALE-FRACTURE AND STRUCTURAL INTEGRITY, 58 (2021) 416-433. doi:10.3221/igf-esis.58.30.
[22]- A. Behtani, S. Tiachacht, T. Khatir, S. Khatir, M.A. Wahab, B. Benaissa, Residual Force Method for damage identification in a laminated composite plate with different boundary conditions. Frattura ed Integrità Strutturale, 16(59) (2022) 35-48. doi:org/10.3221/IGF-ESIS.59.03.
[23]- S. Khatir, S. Tiachacht, B. Benaissa, C. Le Thanh, R. Capozucca, M. Abdel Wahab. Damage Identification in Frame Structure Based on Inverse Analysis. in Proceedings of the 2nd International Conference on Structural Damage Modelling and Assessment: SDMA 2021, 4–5 August, Ghent University, Belgium. Springer. (2022), 197-211. doi:org/10.1007/978-981-16-7216-3_15.
[24]- P. Giannakouras, C. Zeris, Seismic performance of irregular RC frames designed according to the DDBD approach. Engineering Structures, 182 (2019) 427-445. doi:10.1016/j.engstruct.2018.12.058.
[25]- V. SEAOC, Performance based seismic engineering of buildings. Sacramento (CA): Structural Engineers Association of California, USA, (1995).
[26]- M. Slimani, T. Khatir, S. TIACHACHT, D. BOUTCHICHA, B. Benaissa, Experimental sensitivity analysis of sensor placement based on virtual springs and damage quantification in CFRP composite. Journal of Materials and Engineering Structures «JMES», 9(2) (2022) 207-220.
[27]- ATC 40, Seismic evaluation and retrofit of existing concrete buildings. Redwood City (CA): Applied Technology Council. (1996).
[28]- I. Indian Standard, 456 (2000) Indian standard for plain and reinforced concrete code of practice. Bureau of Indian Standards, New Delhi, India.
[29]- I. Standard, Criteria for earthquake resistant design of structures. Bureau of Indian Standards, Part, 1 (1893).
[30]- A. C1621, ASTM C1621 Standard test method for passing ability of self-consolidating concrete by J-ring, ASTM Int. 5 (2014).